Mineralogical Magazine, October 1999, Vol. 63(5), pp. 633–647

Aluminium mass transfer and diffusion in water at 400–550°C, 2 kbar in the K_2O–Al_2O_3–SiO_2–H_2O system driven by a thermal gradient or by a variation of temperature with time

O. VIDAL AND L. DURIN

CNRS URA1316, Département de Géologie, ENS, 24 rue Lhomond, 75231 Paris Cedex 05, France

ABSTRACT

Tube-in-tube experiments involving a time-dependent variation of temperature or a strong thermal gradient were conducted in order to decipher the transport and transfer of Al in a closed medium along with dilute water. Results show that the solubility and the transport of Al are controlled by the alkali availability. Starting from a mixture of kyanite + quartz + muscovite at the hot end of a thermal gradient, Al is transported toward the cold end in the form of a complex with an Al/K stoichiometry close to unity. Since more Al than alkali are released by the dissolution of muscovite, an Al-rich phase (kyanite) forms in the vicinity of the starting minerals undergoing dissolution, although Al is mobile in the system. Then, the variation of the solubility of the Al-K complex with temperature leads to the formation of muscovite (+quartz) at the cold end of the thermal gradient. A quantitative interpretation of the experimental results was carried out using data from the literature on Al speciation in dilute water. Extrapolation of the laboratory data to natural rocks suggests that the diffusion of Al is an efficient transport process under medium-grade, low- to medium-pressure conditions. Therefore, mass-transfer estimates based on mass-balance analyses postulating a fixed Al reference frame should be considered with caution. Also the high fluid to rock ratio calculated from the amount of aluminosilicates occurring in veins of medium-grade metapelites is questionable because such calculations neglect the importance of the transport of Al by diffusion.

KEYWORDS: metapelites, aluminium mass transfer and transport, thermal gradient, aluminosilicates.

Introduction

ALUMINIUM is classically considered to be a slightly mobile or immobile element (Carmichael, 1969; Ferry, 1983; Ague, 1991), and mass transfer studies often assume a fixed Al reference frame. This concept seems to be in agreement with the formation of aluminosilicate segregations after K-bearing minerals by acid leaching (Losert, 1968; Eugster, 1970; Gresens, 1971). In contrast, other authors (Rubenach and Bell, 1988; Yardley, 1977, Foester, 1990, 1991 among others) claimed that the Al_2O_3 component has large mass transfer (the largest according to Foster, 1977) at the thin section scale. The common occurrence of Al silicates in veins within aluminous metasedimentary rocks (see Kerrick, 1990 for a review) also provides convincing evidence for possible Al mobility during metamorphic processes. These contrasting views have important consequences for the determination of mass transport extent at the crustal scale. Indeed, assumptions regarding the mobility of Al are necessary for mass transport studies based on mass-balance analysis as well as for the estimation of fluid amount required to produce a given volume of aluminosilicate-bearing veins (interpreted in terms of infiltration metasomatism, Kerrick, 1990). In view of the very low solubility of Al in pure water at neutral pH, the mobility of Al in aqueous infiltrating fluids is believed to be very low, so that the formation of significant amounts of Al-bearing phases in discordant veins has often been regarded as evidence for very large fluid/rock ratios, a conclusion which has severe implications

for our understanding of metamorphic processes. However, this conclusion is based on the assumption that the diffusive transport of Al is negligible. If the diffusive transport of Al is significant in diluted aqueous solution at realistic *P-T* conditions, Al can be supplied to a vein from the surrounding rock through a virtually stagnant fluid. In this case, the fluid/rock ratios calculated from the amount of aluminosilicate in veins provide little information about the amount of fluid which infiltrated the vein.

The present study was carried out in order to study experimentally the extent of Al diffusion compared to that of Si and K. The basic idea is to induce diffusion by imposing a strong thermal gradient (and therefore chemical potential gradients) within a closed medium. A mixture of muscovite + quartz ± kyanite (representing a rock) is placed at the end of a tube to determine which elements diffuse toward the other end and in which proportion. In addition, another series of experiments was conducted to study the effect of time-dependent temperature variations on the formation of aluminosilicates from a dilute aqueous fluid. This second type of experiment can provide information about the amount of fluid required to produce a given amount of aluminosilicate, muscovite and quartz, comparable to mineral assemblages observed in metapelite veins for a given decrease or increase of temperature. In contrast to more classical isobaric-isothermal dissolution experiments (e.g. Walther, 1986; Woodland and Walter, 1987; Anderson *et al.*, 1987), our approach is based on the analysis of solids crystallizing from the solution, not on the analysis of solution. The solution compositions are calculated *a posteriori* assuming local fluid-solid equilibrium. The results are then interpreted and allow discussion of the modality of transport of Al in a closed system.

Experiments

Experiments were conducted in the K_2O–Al_2O_3–SiO_2–H_2O (KASH) chemical system, using starting mixtures made of natural muscovite (K/Na = 0.93), kyanite and quartz. This mineral assemblage was used because in nature, most of the aluminosilicate segregations or veins observed in medium-pressure metapelites contain muscovite and quartz. Moreover, reaction textures between muscovite and aluminosilicate are common in veins and in the surrounding rocks, suggesting non-isochemical reactions involving fluid-solid interactions. Since only three solid phases are present in the starting mixture, any crystallization of aluminosilicate, muscovite or quartz will also be the result of non-isochemical reactions controlled by the variation of Si, Al and K solubility with temperature. Two kinds of 'tube-in-tube' isobaric experiments (Orville, 1962; Goffé *et al.*, 1988; Robert and Goffé, 1993; Vidal *et al.*, 1995; Poinssot *et al.*, 1996; Vidal, 1997) were performed, in order to study: (1) the transport of Al by diffusion along a thermal gradient; and (2) the fluid-solid transfer of Al between the solids and the fluid resulting from the variation of temperature with time.

The experimental procedure adopted in this study is similar to that described in Vidal (1997). Starting mixtures were made by mixing quartz, muscovite and kyanite in various proportions (Table 1). Minerals were ground under alcohol in an agate mortar to <30 μm and washed with deionized water. The starting charge was sealed in a gold capsule placed in a gold tube containing only deionized water at the beginning of the run. The walls of the capsule were drilled to enable exchange of water (but not of solids) with the tube. In consequence, solids observed outside the capsule at the end of the experiments did crystallize from the solution. If Al is immobile, no Al bearing phase is expected to form outside the capsule. In order to ease the distinction between the starting and the newly formed aluminosilicates, kyanite was used as a starting product, but the experiments were performed outside its equilibrium stability field. In doing so, it was expected that andalusite rather than kyanite would crystallize. Experiments were conducted in cold-seal pressure vessels placed in conventional externally heated, horizontally oriented bombs (in order to avoid the formation of a convection cell in the tube) of the type described by Tuttle (1949). Temperature was measured using a chromel-alumel thermocouple located at the hot end of the bomb and controlled by electronic regulators, and pressure was measured with a Bourdon gauge. Cumulative uncertainties on temperature and pressure measurements were ±6°C and ±100 bar respectively. In order to avoid the formation of metastable phases during the initial period of heating, the rate of heating was rapid (30°C/min.). The temperature overshoot was ~10°C, and the temperature stabilized at the desired value after 15 min.

The experimental conditions are reported in Table 1.

TABLE 1. Experimental conditions and results (P=2 kbar in all the runs)

	Qtz:Ms:Ky (1)	Starting mixture (mg)	H_2O (g)	Run duration (days)	Δpds capsule (2)	XRD	SEM	
	Initial conditions				Results			
							Capsule	Tube
GRL1			1.5	41				
HE	5:1:1	150			50%	No Qtz, Ky/Ms ↑	–	Ky
MP								Amorphous silica
CE	–	–			–	–	–	Ms + Qtz
GRL2			1.5	41				
HE	5:1:1	150			20%	Qtz ↓ Ky/Ms →	–	Amorphous silica
MP								Amorphous silica
CE							–	Ms + Prl + Qtz
GRL14			1.5	53				
HE	2:1:0	70			50%	No Qtz, Ky/Ms ↑	–	Ky
MP								Amorphous silica
CE	2:0:1	70			n.d.	Qtz ↓ Ky/Ms →	Ky dissolves	Illite + Prl + Qtz
T10							Phyllosilicate	
550 → 400°C	4:1:1	25	0.2	55	–	Ky/Ms →	on Ky	Amorphous silica
T12								
400 → 550°C	4:1:1	25	0.2	45	–	Ky/Ms ↑	–	Amorphous silica

(1) Molar proportion in the starting mixture; (2) variation of the capsule weight before and after the experiment.
HE: hot extremity, MP: middle part of the tube; CE: cold extremity.
Ms: muscovite, Qtz: quartz, Prl: pyrophyllite. n.d.: not determined.

Variation of temperature with space (thermal gradient)

One or two capsules filled with the starting mixture were placed at the hot (HE) or/and the cold end (CE) of a 15 cm long gold tube containing 1.5 g of water. In order to trap the newly-formed products at their position of crystallization and to prevent their displacement during the opening of the autoclave, the outer tube was accordion-shaped (Vidal, 1997). The thermal profile along the tube (from 550°C at the HE to 400 ± 15°C at the CE, Fig. 1) was calibrated using three thermocouples, successively placed at the HE, at 5 cm, and then at 10 cm from the HE of a tube filled with water. The thermal profile was interpolated between these three measures of temperature and extrapolated toward the cold extremity of the tube.

At the end of the run, quench from 550 to 80°C was achieved in 6 min. using a compressed air jet. The autoclave was then cooled to 15°C by immersion in cold water. After quenching, freezing of the solution by immersion in liquid nitrogen prevented solid movements during opening. The tube was then cut in six 2 cm-long pieces. These pieces were placed in an oven and heated at 90°C for 1 h to evaporate the solution. The walls of the tube pieces were then examined with a scanning electronic microscope (SEM) equipped with an X-ray analyser for EDS

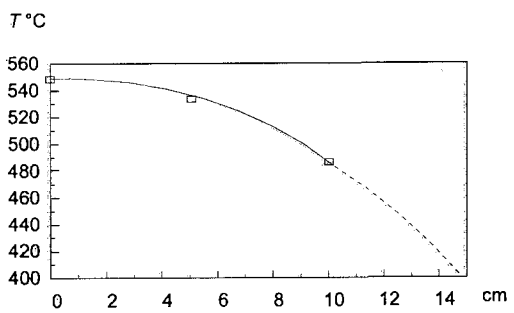

FIG. 1. Thermal profile along the tubes. Squares indicate the temperatures measured for the calibration of the thermal gradient.

analyses, in order to identify solids precipitated from the solution. Comparison of the X-ray diffraction (XRD) patterns obtained from the solids in the capsule, before and after the experiment, allowed semi-quantitative estimates of the variation of quartz:muscovite:kyanite proportions.

Variation of temperature with time

Twenty five milligrammes of the starting mixture was enclosed in a 1 cm long, 2 mm diameter capsule. The capsule was enclosed in a 4 cm long, 3.2 mm diameter tube with 200 µl of distilled water. The tube was welded shut and placed in the zone of minimal thermal gradient of the autoclave. The initial temperature conditions were maintained for one week, in order to achieve solid-solution equilibrium. Then, the temperature was changed by 20°C every week. The temperature stabilized at the new conditions after 1 h when the temperature was decreased, and in <10 min. when the temperature was increased. The pressure was then adjusted to 2 kbar.

Results

Tubes in a thermal gradient

The results are reported in Table 1 and described below. Five newly formed solid phases are detected; namely pyrophyllite, quartz, kyanite, siliceous amorphous products and mica (muscovite and illite composition). The location of these phases in the tube is related to the temperature conditions. Scanning electron microscopy (SEM) examination of the tube walls indicates that the amount of newly-formed solids increases abruptly over the colder 3 cm of the tube. X-ray diffraction shows that quartz is completely removed from all capsules located at the HE.

GRL1

Comparison of the capsule weight before and after the run indicates that half of the starting mixture was removed. The observations by SEM suggest that muscovite and kyanite both dissolved, and XRD indicates that the proportion of remaining kyanite increases relative to muscovite, i.e. the dissolution of muscovite is more important than that of kyanite. In the tube, in the vicinity of the capsule, small new euhedral grains of aluminosilicate composition are observed over the first 2 cm (Fig. 2*a*). It was not possible to determine whether these grains are kyanite or andalusite from the SEM observations, and attempts at collecting them for XRD determination failed. From the hot to the cold end, amorphous silica occurs in the form of a continuous film which is <0.5 µm thick (Fig. 2*a*). It shows a typical habitus previously observed by Vidal *et al.* (1995) and Vidal (1997) and is interpreted as a quenching product. Muscovite (Si/Al = 0.91–1.02, Si/K = 3.1–3.5 from five EDS analyses) and quartz appear abruptly at the CE, and cover the last 2 cm (Fig. 2*b*).

GRL2

Quartz is partly removed from the capsule whereas the proportion of kyanite and muscovite remains constant. The overall material loss from the capsule during the experiment is <20 wt.%. Well-crystallized euhedral pyrophyllite grains are observed in the tube, in the vicinity of the capsule (Fig. 2*c*). Toward the HE, the abundance of siliceous amorphous material covering the tube walls made it impossible to detect other crystalline phases using the SEM. Material was collected from the 3 last cm of the HE and immersed in 1/5 diluted fluoridric acid (40%) to dissolve the amorphous products (Brown and Fyfe, 1971). The solution was then filtered using a 2 µm filter. A few grains (probably andalusite or kyanite, which are not dissolved by HF) were observed, but could not be collected for SEM observation.

GRL14

About half of the material (all quartz) is removed from the capsule at the HE. As with GRL1, newly formed aluminosilicate grains are observed in the vicinity of the capsule at the HE. As shown in Fig. 2*d*, some of these grains exhibit step-like features caused by perfect 100 cleavage (or lamellar twinning?), and good 010 cleavages which are typical of kyanite rather than andalusite. Amorphous products cover the walls of the middle portion of the tube. Mixed quartz and phyllosilicates of illite composition (Si/Al = 1.45–1.57, Si/K = 6–8 from five EDS analyses) crystallized at the CE (Fig. 2*e*). In the capsule located at the CE, quartz and kyanite are still present in the capsule, but the kyanite grains exhibit strong features of dissolution (Fig. 2*f*).

Variation of temperature with time

No solid phases other than amorphous silica are observed on the wall of the tube in either

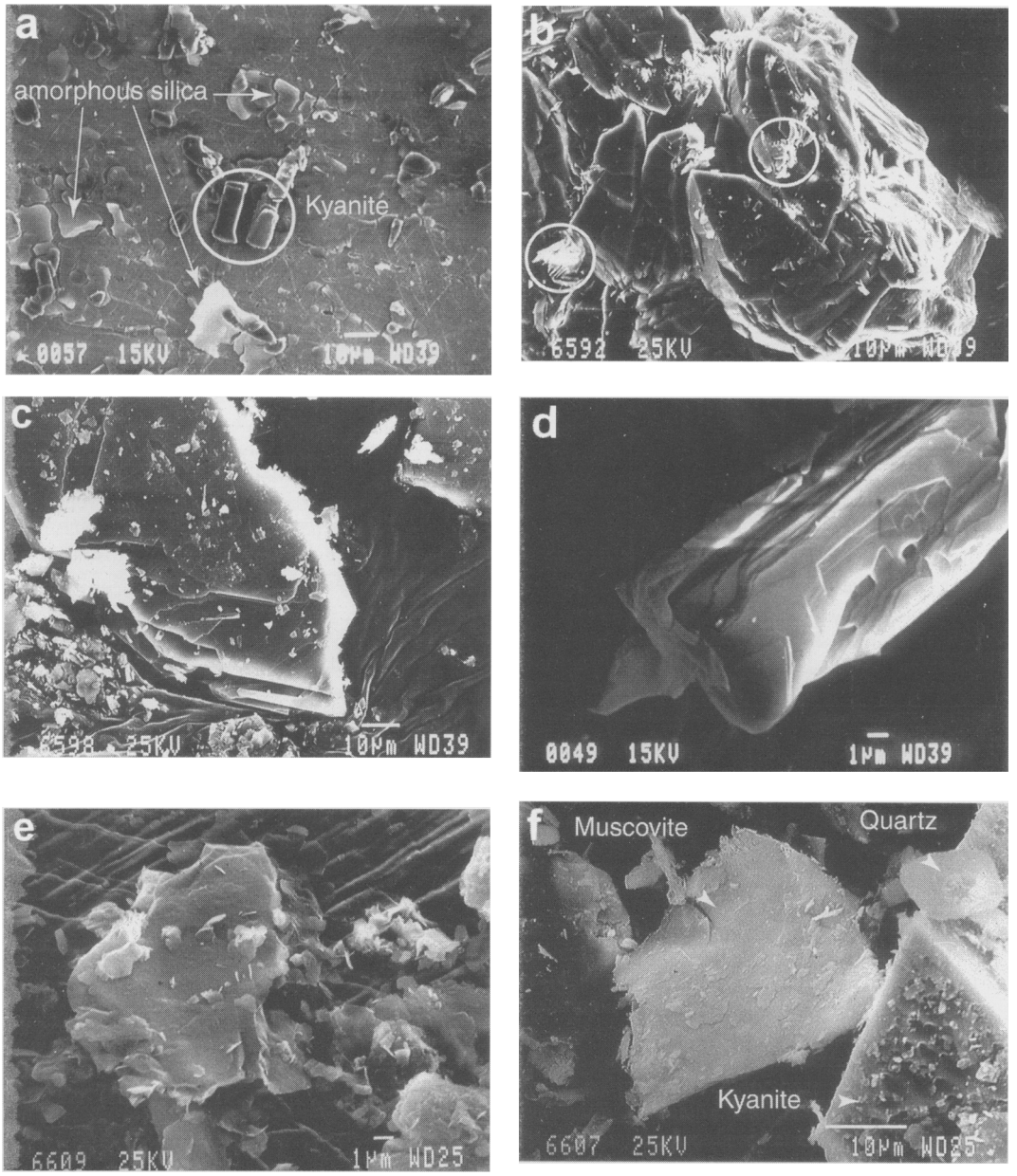

FIG. 2. Scanning electron micrographs of minerals that crystallize in the tubes GRL1 and GRL14. GRL1: (*a*) Newly formed aluminosilicate (probably kyanite) and amorphous silica at the hot end; (*b*) quartz and muscovite (circled) at the cold end; GRL2: (*c*) pyrophyllite crystallizing at the cold end; GRL14; (*d*) euhedral kyanite grain with a step−like structure caused by perfect 100 cleavage or lamellar twinning and good 010 cleavage; (*e*) phyllosilicate of illite composition crystallizing at the cold end; (*f*) starting kyanite grain with an irregular surface (dissolution feature) in the presence of quartz and muscovite, in the capsule at the cold end.

experiment. For the experiment involving an increase of temperature with time (T12), SEM observations of the solids in the capsule are difficult to interpret, and do not provide a clear indication of which phase dissolved and which crystallized. No variation of the muscovite/kyanite proportion is indicated by XRD. In the case of T10, kyanite starting grains are sometimes covered by thin lamellae of new phyllosilicates that could not be analysed. The XRD results indicate that the proportion of kyanite increases slightly relative to that of muscovite in the capsule.

Interpretation

Importance of ordinary diffusion vs thermodiffusion

In the experiments conducted under a thermal gradient, mass transfer (dissolution of the starting products and precipitation of secondary products in the tube) and mass transport from one end of the tube to the other are controlled by the temperature variations with space. A flux of matter occurs in order to reach equilibrium, i.e. to make the chemical potential of each component uniform throughout the solution submitted to a thermal gradient. In a system with no reaction, the flux of any species i along the tube can be expressed as the sum of the fluxes resulting from Fickian diffusion (concentration gradients) and thermal diffusion (thermal gradient) (see Vidal and Murphy, 1999 and references therein for more details)

$$J_i = -D_i \frac{dC_i}{dx} + C_i D_i' \frac{dT}{dx} \qquad (1)$$

with D = diffusion coefficient, C = concentration, x = distance along the tube and D′ = thermodiffusion coefficient. At the beginning of the run, solids dissolve in the capsule, and aqueous species diffuse into the tube. Then, the flux resulting from chemical diffusion is balanced by the flux resulting from thermal diffusion. Assuming that the thermal profile along the tube is linear, the steady state concentrations of any dissolved species at the hot (C^H) and cold (C^C) extremities are related by the simple expression:

$$\frac{C_i^H}{C_i^C} = \exp\left(\frac{D_i'}{D_i}(T^C - T^H)\right) \qquad (2)$$

The ratio D′/D (known as the Soret coefficient) is positive for most species (Schott, 1973; Thornton and Seyfried, 1983; Costesèque, 1985), so that at steady state conditions, the concentration of dissolved species should be higher at the CE than at the at the HE. However, the Soret coefficients are small (of the order of 1×10^{-3}°C^{-1}) so that the concentration differences between the two extremities (ΔC) of the tube are small. For example, Watson and Wark (1997) found that for SiO_2, ΔC_{SiO2} <5% for ΔT = 80°C at $T_{average}$ = 860°C. For this reason, it is assumed in the following that the influence of thermal diffusion is negligible, and that Fickian diffusion alone tends to make the concentration of dissolved species homogeneous throughout the tube. Depending on the variation of the solubility products with temperature, supersaturation is achieved toward the cold or the hot end of the tube, and new phases crystallize. Once nuclei have formed, concentration and chemical potential gradients acting as driving forces for mass transport form between the capsule and the tube, and between the HE and the CE. This is shown well in runs GRL1 and GRL14 by the complete removal of quartz from the capsules located at the HE and its crystallization at the CE (the solubility of quartz decreases with temperature).

The role of speciation in the transport of Al in solution

The crystallization of muscovite at the CE in GRL1 indicates that Al and K also migrate down the thermal gradient. However, the presence of newly formed kyanite at the HE of GRL1 and GRL14, and the absence of such an Al-rich phase at the CE of these tubes shows that the transport of Al from the hot to the cold end is limited. The same observation was made for similar experiments conducted in the Na_2O-Al_2O_3-SiO_2-H_2O (NASH) system (Vidal, 1997). Hence, a general trend observed in the K/NASH system is the formation of assemblages more aluminous than the starting mixture at the HE of the gradient and more siliceous at the CE.

This observation is consistent with the results of Anderson and Burnham (1983), Walther (1986), Woodland and Walter (1987) and Anderson *et al.* (1987) which indicate that in the systems NASH and KASH, the molality of Al is close to that of alkali and a (Na,K)-Al complex is the dominant Al species in aqueous solution. According to Anderson *et al.* (1987), this complex can be written $(K,Na)Al(OH)_4$. In the NASH system, Anderson and Burnham (1983) showed that the fraction (p) of total Na complexed with Al is likely to decrease from 0.9 at 700°C to 0.74 at

500°C. In the KASH system, Pascal (1984) and Anderson *et al.* (1987) suggested that p is ~0.85 at 500 and 600°C. At lower temperature, p is unknown, but it can be approximated to $p = 0.6$ by extrapolating the Al/K stoichiometry reported by Anderson *et al.* (1987) in the 550–700°C range to 400°C. More Al than alkali is released by the dissolution of muscovite, so that whatever the exact value of p, less than half of the Al released is complexed with K and can be transported. The remaining uncomplexed Al reacts with dissolved silica to form kyanite at the HE of the tubes GRL1 and GRL14. Similarly, pyrophyllite or even diaspore formed at the HE of the tubes in the experiments conducted in the NASH system (Vidal, 1997). It is emphasized that the presence of kyanite close to but outside the capsule in GRL1 and GRL14 (kyanite certainly crystallized inside the capsule too, but it was impossible to differentiate secondary from primary minerals with the SEM) implies that uncomplexed Al could also be transported over short distances. However, our experimental results suggest that the transport of Al in the form of $KAl(OH)_4$ is more efficient.

Estimation of solution compositions and amount of newly formed minerals

Experiments under thermal gradient

A more quantitative interpretation of the experimental results requires an estimation of the solution composition throughout the tube. Assuming the rate of reactions to be limited by mass transport rather than by mass transfer kinetics (Goffé *et al.*, 1988; Vidal, 1997), heterogeneous local equilibrium between minerals and aqueous species (Korzhinskii, 1959) was probably closely approached in our experiments. Thus, the composition of the solution at 550°C (HE) and 400°C (CE) can be approximated following the procedure described in the Appendix. The difference between the composition of the solution at the HE and the CE was then used to calculate the proportion of quartz, muscovite and kyanite that dissolved and that formed at both ends of the tube.

Results of the calculations are reported in Table 2. In the capsule containing 0.15 g starting mixture at the beginning of the experiment, the dissolution of all quartz (89×10^{-5} mol) through reaction R1 (cf. Appendix):

$$\text{Starting mixture} \rightarrow a\text{Ky} + b\text{Ms} + S(\text{solution})_{\text{MKQ}}^{550\,^{\circ}\text{C}} \qquad \text{(R1)}$$

is accompanied by the dissolution of 36×10^{-6} mol. muscovite and the precipitation of 39×10^{-6} mol. kyanite. As a result, the kyanite to muscovite molar proportion at the HE increases from 1 to 1.5. A further dissolution of muscovite would require the crystallization of a new phase more aluminous than kyanite (corundum), which was not observed in our run products, but that should appear for longer run duration or different starting mixture compositions (Vidal, 1997). Figure 3 depicts the phase relations observed among the starting mixtures, the newly formed products and the solution. In the case of GRL1, the evolution of the Si:K:Al molar proportion defined by solids at the HE during (R1) is shown by the open arrow. When all quartz is removed from the HE, $\sim 50 \times 10^{-5}$ mol. quartz and 38×10^{-7} mol. muscovite should have crystallized at the CE through the reaction R2 (cf. Appendix):

$$S(\text{solution})_{\text{MKQ}}^{550\,^{\circ}\text{C}} \rightarrow c\text{Ms} + d\text{Qtz} + S(\text{solution})_{\text{MQ}}^{400\,^{\circ}\text{C}} \qquad \text{(R2)}$$

These quantities, although very small are detectable by SEM examination of the tube wall. They correspond to 1×10^{-2} and 53×10^{-5} cm^3 respectively. The experiments were not designed to allow precise determination of the Ms:Qtz proportion. However, analysis of the SEM micrographs of the run products indicates that the volume of quartz crystallizing at the CE of GRL1 was 10 to 50 times that of muscovite. These values are in broad agreement with the Qtz:Ms volume ratio (20) calculated from the solution composition reported in Table 2. If calculations are performed with $p = 0.7$ instead of 0.6 at 400°C, Qtz:Ms = 35. Therefore, experiments with the purpose of obtaining more accurate Qtz:Ms proportions at the CE should provide opportunities to further constrain the less reliable thermodynamic data listed in Table 2.

As shown in Fig. 3, the fraction of dissolved material is significant compared to that in solids, so that mass balance constraints are not strictly obeyed when considering only the solid phases, i.e. the newly formed products at both ends of the tube and the starting mixture are not connected by a single tie-line (in contrast to the assumption made by Vidal, 1997).

Using the same procedure of calculation as for GRL1, we also calculated the solution composition and the molar proportions of solids at the HE and the CE of GRL14. The Al concentration, buffered by the presence of kyanite at the CE is greater than at the CE of GRL1, where kyanite

TABLE 2. Calculated composition of the solution in equilibrium with Musc + Ky + Qtz (MKQ) or Musc + Qtz (MQ) and of the amount of solids precipitating from the solution at the extremities of the tubes

	550MKQ	400MQ	550MKQ	400MKQ
$Log[H_4SiO_4]_{Qtz}$	−1.052	−1.384	−1.052	−1.384
$Log[Al(OH)_3]_{Crn}$	−4.050	−4.100	−4.050	−4.100
ΔG_{E1}	314	1914	314	1914
ΔG_{E2}	−60908	−38660	−60908	−38660
LogKKOH	−1.981	−1.297	−1.981	−1.297
$LogKH_2O$	−10.370	−9.850	−10.370	−9.850
p = Al/K	0.850	0.600	0.850	0.600
$aSiO_2$	1.000	1.000	1.000	1.000
aAl_2O_3	0.955	0.151	0.955	0.710
aKy	1.000	0.212	1.000	1.000
$Log[Al(OH)_3]$	−4.060	−4.511	−4.060	−4.174
$Log(K^+/H^+)$	3.865	4.009	3.865	3.000
pH	7.118	6.930	7.118	6.425
$Log[K^+]$	−3.253	−2.920	−3.253	−3.425
Log$a$KOH	−4.524	−4.544	−4.524	−5.553
$LogKAl_p(OH)_4$	−2.560	−2.753	−2.560	−3.398
Log[Al]total	−2.546	−2.745	−2.546	−3.331
Log[K]total	−2.475	−2.523	−2.475	−3.109
Log[Si]total	−1.052	−1.384	−1.052	−1.384

	GRL1		GRL14	
	R1	R2	R1	R3
pds sol (g) (1)	10.8		7.3	
$S \times 10^5$	3.6	3.2	2.4	0.57
Qtz $\times 10^5$ (mol.)	−89	50 (*d*)	−60	29 (*d*)
Ms $\times 10^{-5}$ (mol.)	−3.6 (*b*)	0.38 (*c*)	−2.4 (*b*)	1.9 (*c*)
Ky $\times 10^5$ (mol.)	3.9 (*a*)	0	2.6 (*a*)	−1.9 (*e*)
F/R(weight) (2)	72	355	48	392
F/R (vol.%) (2)	216	1070	145	1200

(1) Apparent weight of solution that would be required to dissolve all quartz from the capsule at 550°C, 2 kbar. (2) Apparent fluid:rock ratio calculated assuming that the mineralogical changes at both extremities of tube and in the capsule(s) result from the percolation of a solution from the hot to the cold extremity (single pass model).
S, *a*, *b*, *c*, *d* and *e* refer to the stoichiometric coefficients for reactions R1, R2 and R3 listed in the Appendix.

was absent. The difference in Al solubility between the HE and the CE is of the same magnitude as the difference in K solubility (Table 2). However, since three Al are required for one K to form muscovite, kyanite must dissolve from the capsule at the CE. Assuming that only muscovite and quartz formed at the CE through reaction R3 (cf. Appendix),

$$S(\text{solution})^{550°C}_{MKQ} + e\text{Ky} \rightarrow c\text{Ms} + d\text{Qtz} + S(\text{solution})^{400°C}_{MKQ} \quad \text{(R3)}$$

~1 mol. kyanite must dissolve for 1 mol. muscovite and 30 mol. quartz precipitating, respectively. Actually, pyrophyllite was also observed to form in GRL14, so that the amount of dissolved kyanite should be higher.

Experiments involving a time-dependent variation of temperature

The compositions of solution calculated above can also be used to predict the amount of kyanite, muscovite and quartz that should dissolve or form in

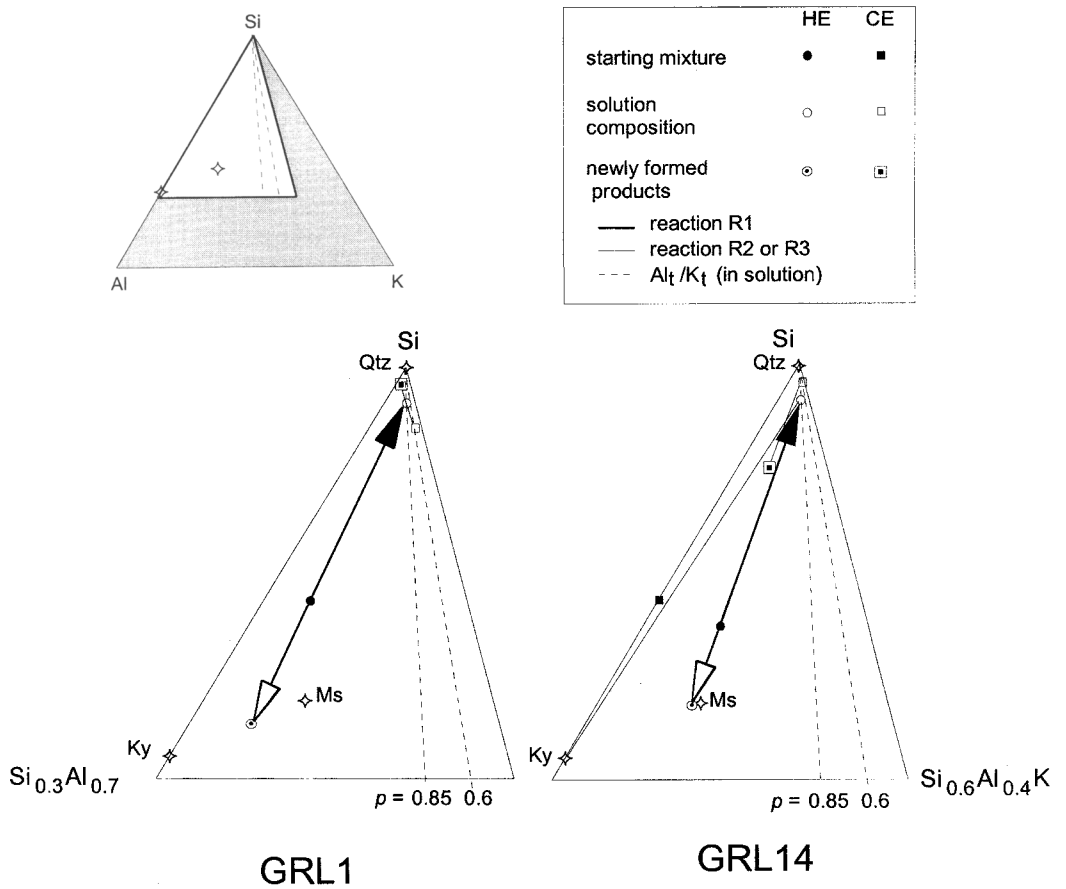

FIG. 3. Ternary plot of the system K_2O-Al_2O_3-SiO_2 projected from H_2O onto the anhydrous base. Kyanite (Ky): $SiAl_2O_5$; muscovite (Ms) $KAl_3Si_3O_{10}(OH)_2$; quartz (Qtz): SiO_2. The compositions of solution calculated as indicated in the appendix are listed in Table 2. The compositions of the starting mixtures are listed in Table 1. The open arrows connect the starting and the final compositions (resulting from the reaction R1 given in the Appendix) of the mixture in the capsule located at the hot end of the tubes. The filled arrow indicates the composition of the solution in equilibrium with the muscovite + quartz + kyanite mixture at the hot end. The thin tie line corresponds to the reactions R2 (GRL1) or R3 (GRL14) given in the Appendix. The composition of the solution at the hot extremities lies on the dotted line labelled p (=Alt/Kt) = 0.85 whereas that of the solution at the cold end lies on the dotted line labelled p = 0.6.

experiments T10 and T12. The results are listed in Table 3. They indicate that during the first week in which temperature was held constant, 6.7×10^{-7} mol. muscovite and 1.65×10^{-5} mol. quartz dissolved and 7.19×10^{-5} mol. kyanite precipitate to achieve equilibrium between the muscovite + quartz + kyanite assemblage and solution at 550°C. Then, the variation of the solution composition with decreasing temperature from 550 to 400°C led to the formation of ~5.13×10^{-7} mol. muscovite and 8.5×10^{-7} mol. quartz, together with the dissolution of 5.32×10^{-7} mol. kyanite. These quantities are 30 times lower than that of muscovite and quartz calculated above for the CE of GRL1. Moreover, in contrast to the experiments conducted under thermal gradient, at least part of the newly formed products crystallized inside the capsule. Consequently, it is not surprising that new secondary products were not detected on the tube wall during SEM examination. If 80% of kyanite that forms during the initial equilibration of the solution (first week) crystallized in the capsule, the Ms:Ky

TABLE 3. Calculated amount of solids dissolved and formed in the experiment involving a variation of temperature with time

	T10			T12		
	First week (T = 550°C)	550 → 400°C	Total	First week (T = 400°C)	400 → 550°C	Total
Qtz × 10^5 (mol.)	−1.64	0.85	−0.79	−0.79	−0.85	1.64
Ms × 10^7 (mol.)	−6.69	5.13	−1.56	−1.56	−5.13	−6.69
Ky × 10^7 (mol.)	7.19	−5.32	1.86	1.86	5.32	7.19

volumic ratio in the capsule is calculated to decrease by 6% in T10 and by 1% in T12. This explains why even though the SEM examination was not conclusive, the XRD of solids in the capsule showed a slight decrease of the Ms:Ky peak intensities in the case of T10 and no variation in the case of T12.

Discussion

Aluminosilicate segregations: a source of dissolved Al

Our results confirm the observations of Anderson and Burnham (1983), Walther (1986), Woodland and Walter (1987) and Anderson *et al.* (1987) on the solubility of Al in alkali-bearing systems. In aqueous fluids of low salinity, in the absence of additional complexing elements, the solubility and the transport of Al is controlled by the alkali availability. Consequently, dissolution of minerals with an Al/K stoichiometry >1 will lead to the formation of an Al-rich segregation. This result is consistent with the occurrence of aluminosilicates nodules and segregation formed after K-bearing minerals (Losert, 1968; Gresens, 1971; Fisher, 1970). Therefore, we suggest that Al-rich segregations can form although Al is a mobile component, and that the ionic reactions and the Al-constant frame postulated by Losert (1968), Gresens (1971) and Fisher (1970) to model the genesis of the nodule is questionable. In fact, aluminosilicate segregations should form because they are a source of dissolved alkali-complexed Al. In this case, the relative Al enrichment in the segregation is simply due to the preferential loss of other elements that are soluble in the uncomplexed form. A similar hypothesis has been made by Dipple *et al.* (1990) who showed that in spite of the loss of Al from the Hunts Brook fault zone, the sillimanite-bearing fault rocks are more aluminous than the Rope Ferry Gneiss from which they were derived.

Transport by diffusion and fluid:rock ratio estimates

In the case of aluminosilicate-bearing veins believed to result from infiltration metasomatism (Kerrick, 1990), the low Al concentrations in aqueous fluids measured experimentally implies that enormous volumes of infiltrating fluid are involved in their formation. This can be illustrated using our experimental results and the values reported in Table. 2. The coefficient S in R1 allows the quantity of pure water needed to dissolve all of the quartz at the HE of GRL1 and GRL14 to be calculated. From the composition of the solution equilibrated at 550°C with muscovite + quartz + kyanite, it appears that 10.8 g of water are necessary for 0.15 g starting mixture, corresponding to a minimum fluid/solid volume ratio of ~216. If we now postulate that muscovite + quartz formed at the CE of GRL1 from a fluid moving in single pass down temperature (like an ascending fluid percolating a crack network), the calculated fluid/solid ratio is 1200 when using the Si solubility at 400°C, and 12,000 when using the solubility of $Al(OH)_3$. These ratios clearly have no meaning when transport occurs only by diffusion, as is the case in our experiments. However, they suggest that: (1) an extremely high and unrealistic fluid/solid ratio can always be calculated, even in a completely closed system; and (2) these ratios are very dependent on which mineral or element they are based. Similar problems occur when considering natural vein assemblages formed in pelites metamorphosed in a regional medium-grade, medium-pressure metamorphic context, and the significance of the fluid/rock ratio based on mineral assemblages in veins is highly questionable. Moreover, some authors have argued that even in fractured rocks, fluid circulation may not be always possible at P > a few kbar (Furlong *et al.*, 1991; Hanson, 1992; Cesare, 1994). In these cases, high fluid/rock ratios and the crystallization of alumino-silicate in

veins formed by hydrofracturing cannot be interpreted in terms of fluid infiltration alone, even when postulating the existence of very aggressive fluid compositions.

Transport by diffusion is an alternative or additional process that is generally ignored when dealing with distance of transport of more than a few mm, but it deserves consideration. The diffusion of K-complexed Al in response to a chemical potential gradient has proven to be an efficient and rapid process in our experiments. In natural systems, such chemical potential gradients are believed to exist from the thin section scale (Foester, 1990; 1991) to the metre scale (Cesare, 1994). Diffusive transport over kilometre distances has so far not been demonstrated for Al, but it is likely to be possible. For comparison, Watson and Wark (1997) showed experimentally that the diffusivity of silica in response to a thermal gradient is much more significant than predicted by calculation. The diffusive transport of silica in a 20°C/km geotherm may occur on the kilometre scale per My. Although additional experiments aimed to determine the diffusivity of Al at various *P-T* conditions are required, our preliminary data suggest that as for silica, the diffusivity of Al could be more important than is generally admitted. The case in which Al diffusion through an intergranular fluid could be significant at the metre scale is a crucial issue when estimating fluid/rock ratios from the vein's mineralogy and abundance. If the diffusion of Al is significant compared to other long-distance transport mechanisms, Al transport from the host rock to the vein can occur through a virtually stagnant fluid and fluid/rock ratios calculated from the abundance of aluminosilicate in veins are meaningless. These ratios may be much lower than calculated when assuming that advection/convection is the sole mechanism of transport.

Formation of aluminosilicate bearing veins in a closed system in P-T evolution

In contrast to our experiments, strong thermal gradients do not exist between the veins and the host rock in nature. It is also unlikely that the pressure gradient can be maintained over a period long enough to promote significant chemical potential gradients. Therefore, in the cases in which the circulation of large fluid amounts is proved to be unrealistic, the formation of aluminosilicate-bearing veins should result from the variation of temperature and/or pressure with time. The time-dependant variations of temperature and pressure have two effects that may enhance the crystallization and growth of aluminosilicates in veins.

(1) Variation of the fluid composition buffered by one mineralogical assemblage.

It has been suggested that aluminosilicates may form in veins in response to the variation of the solubility products with a decrease of temperature (Goffé *et al.*, 1987). However, our experiments involving a variation of temperature with time indicate that the amount of aluminosilicate or muscovite crystallizing this way was too low to be detected. Moreover, using the fluid compositions determined above, we calculate that in a rock containing 10 vol.% fluid whose composition is buffered by the muscovite + kyanite + quartz assemblage in 1:1:10 molar proportion, ~40 cm^3 muscovite and 100 cm^3 quartz should precipitate per m^3 of rock for a temperature decrease from 550 to 400°C, whereas ~18 cm^3 kyanite should precipitate with increasing temperature. These volumes represent a small fraction of the total rock volume. This suggests that in a closed system, significant amounts of aluminosilicates in veins cannot crystallize in response to the variation of the solution composition with temperature. The effect of pressure variations is also believe to be too weak because: (a) Al complexing by alkalis is pressure independent (Anderson and Burnham, 1983); and (b) although the solubility of Al in KNASH may increase significantly with pressure (Adcock and MacKenzie, 1981; Davis, 1972) it always remains low. Repeated pressure variations by tectonic pumping may play a role in the vein's genesis, but the magnitude of Al solubility variations is certainly too low to account for large amounts of mineral precipitating through this mechanism. Therefore, in the cases in which the circulation of large fluid amounts is proved to be unrealistic, the formation of large amounts of aluminosilicates in veins requires the transport of Al from the host rock.

(2) Variation of the host rock mineralogy

The diffusion of Al from the adjacent rock to the vein is driven by chemical potential gradients that can be due to chemical gradients. As discussed extensively in the literature (see Foster, 1990; 1991 and reference therein), such chemical potential gradients exist at the thin section scale between reactants and products of a

reaction resulting from the variation of temperature and/or pressure conditions. As postulated by Cesare (1994), chemical potential gradients should also form at the centimetre to metre scale. When a reaction responsible for a mineralogical change in a rock (when an isograd is crossed) involves the destabilization of Al-bearing minerals, there is a local production of Al which dissolves and migrates in the surrounding fluid. For energy reasons, nucleation of the product of reaction on the strained minerals at vein walls is favoured (Lasaga, 1981; Carlson, 1989). Then, chemical potential gradients between the reactants (production of elements) and the products (consumption of elements) will drive diffusion from the rock towards the vein. Depending on which reaction occurs in the rock, such a process (synmetamorphic veining; Cesare, 1994) may lead to the formation of aluminosilicate $\pm$ quartz veins in a closed system without specific requirement for fluid circulation, temperature or pressure gradient. As long as the reactants are present in the rock, and in the absence of an overwhelming reaction, Al will be supplied continuously to the vein. Significant amounts of elements might be transported this way, leading to the formation of significant amounts of aluminosilicates, even if the solubility of Al is low.

Conclusion

Results of the tube-in-tube experiments reported here confirm previous observations concerning the control by alkalis of the Al solubility and mass transport in the KASH system. In a system where the fluid composition is buffered by the rock, the fraction of dissolved Al (in the form of a complex with an Al/K stoichiometry close to 1) depends on the availability of complexing alkalis. Thus, at given pressure and temperature conditions, the amount of dissolved Al should depend on the bulk rock composition. In nature, other complexing elements may exert an important control on the solubility of Al. For example, Vard and Williams-Jones (1993) reported an Al concentration as high as 1 wt.% in fluid inclusions of vug minerals in dawsonite ($NaAl(OH)_2CO_3$)-altered phonolite. The authors proposed that high concentrations of bicarbonate/carbonate and fluoride may have led to the formation of highly soluble Al complexes. The occurrence of muscovite instead of K-feldspar in quartz-aluminosilicate-muscovite segregations is also indicative of CO_2-bearing fluids (Poty, 1969; Sauniac and Touret, 1983). Preliminary experiments done with muscovite-quartz-kyanite + calcite starting mixtures indicate that the transport of Al is indeed dramatically increased in HCO_3^- bearing fluids.

Consequently, mass balance studies suggesting an Al-constant reference frame or fluid/rock ratio estimates relying on the solubility of Al in pure water combined with the amount of aluminosilicates in veins should be considered with caution.

Moreover, our data suggest that the transport of Al by diffusion could be more important than is generally admitted. If the diffusion of Al is significant in comparison to other long-distance transport mechanisms, Al mass transport from the host rock to the vein can occur through a virtually stagnant fluid and the fluid/rock ratios calculated from the abundance of aluminosilicate in veins are meaningless. These ratios may be much lower than calculated when assuming that advection/convection is the sole mechanism of transport.

Acknowledgements

Thanks are due to W.M. Murphy and C. Poinssot for helpful discussions, and to J. Touret for his review. We are also grateful to M.-C. Magonthier for her assistance during the SEM work at the CEA/DCC/DESD/SESD-CEN-FAR, and to N. Catel and G. Marolleau for their help during the experiments. Suggestions by C. Chopin and D. Pissarenko improved an earlier version of the manuscript. This work was supported financially by the DBT II-INSU programme 'Fluide dans la crôute'.

References

Adcock S.W. and MacKenzie, W.S. (1981) The solubility of minerals in supercritical water. In *Progress in Experimental Petrology* (C.E. Ford, ed.), Fifth progress report of research supported by N.E.R.C., **5**, 9–10.

Ague, J.J. (1991) Evidence for major mass transfer and volume strain during regional metamorphism of pelites. *Geology*, **19**, 855–8.

Anderson, G.M. and Burnham, C.W. (1983) Feldspar solubility and the transport and the of aluminium under metamorphic conditions. *Amer. J. Sci.*, **238A**, 283–97.

Anderson, G.M., Pascal, M.L. and Rao, J. (1987) Aluminium speciation in metamorphic fluids. In *Chemical transport in metasomatic processes* (H.C. Helgeson, ed.), D. Reidel Publishing Company,

Dordrecht, pp. 297–321.

Berman, R.G. (1991) Thermobarometry using multi-equilibrium calculations: a new technique, with petrological applications. *Canad. Mineral.*, **29**, 833–55.

Brown, G.C. and Fyfe, W.S. (1971) Kyanite-andalusite equilibrium. *Contrib. Mineral. Petrol.*, **33**, 227–331.

Carlson, W.D. (1989) The significance of intergranular diffusion to the mechanism of porphyroblast crystallization. *Contrib. Mineral. Petrol.*, **103**, 1–24.

Carmichael, D.M. (1969) On the mechanism of prograde metamorphic reactions in quartz-bearing pelitic rocks. *Contrib. Mineral. Petrol.*, **20**, 244–267.

Cesare, B. (1994) Synmetamorphic veining: origin of andalusite-bearing veins in the Vedrette di Ries contact aureole, Eastern Alps, Italy. *J. metam. Geol.*, **12**, 643–53.

Costesèque, P. (1985) Sur la migration des éléments par thermodiffusion. Etat et perspectives d'un modèle géochimique. *Bull. Minéral.*, **108**, 305–24.

Davis, N.F. (1972) *Experimental studies in the system sodium-alumina trisilicate-water: part I: the apparent solubility of albite in supercritical water.* Unpublished Ph.D. thesis, Pennsylvania State University, 332 p.

Dipple, G.M., Wintsh, R.P. and Andrews, M.S. (1990) Identification of the scales of differential element mobility in a ductile fault zone. *J. metam. Geol.*, **8**, 645–661.

Eugster, H.P. (1970) Thermal and ionic equilibria among muscovite, K-felspar and aluminosilicate assemblages. *Fortschr. Mineral.*, **47**, 106–23

Ferry, J.M. (1983) On the control of temperature, fluid composition, and reaction progress during metamorphism. *Amer. J. Sci.*, **238-A**, 201–32.

Fisher, G.W. (1970) The application of ionic equilibria to metamorphic differentiation: an example. *Contrib. Mineral. Petrol.*, **29**, 91–103.

Foster, C.T. (1977) Mass transfer in sillimanite-bearing pelitic schists near Rangeley, Maine. *Amer. Mineral.*, **62**, 727–46.

Foster, C.T. (1990) Control of material transport and reaction mechanisms by metastable mineral assemblages: an example involving kyanite, sillimanite, muscovite and quartz. In *Fluid-mineral Interactions: a tribute to to H.P. Eugster* (R.J. Spencer and I-Ming-Chou, eds), The Geochemical Society, Spec. Publ., **2**, 121–32.

Foster, C.T. (1991) The role of biotite as a catalyst in reaction mechanisms that form sillimanite. *Canad. Mineral.*, **29**, 943–63.

Furlong, K.P., Hanson, R.B. and Bowers, J.R. (1991) Modeling of thermal regimes. *In Contact metamorphism* (D.M. Kerrick, ed.), *Reviews in Mineralogy*, Mineralogical Society of America, Washington, D.C., **26**, pp. 437–506.

Goffé, B., Murphy, W.M. and Lagache, M. (1987) Experimental transport of Si, Al and Mg in hydrothermal solutions: an application to vein mineralization during high-temperature, low pressure metamorphism in French Alps. Contrib. Mineral. Petrol., **97**, 438–50.

Gresens, R.L. (1971) Application of hydrolysis equilibria to the genesis of pegmatite and kyanite deposits in the northern New Mexico. *Mountain Geologist*, **8**, 3–16.

Hanson, R.B. (1992) Effect of fluid production on fluid flow during regional and contact metamorphism. *J. metam. Geol.*, **10**, 87–97.

Kerrick, D.M. (ed.) (1990) The Al_2O_5Si polymorphs. *Reviews in Mineralogy*, **22**, Mineralogical Society of America, Washington, D.C., 406 p.

Korzhinskii, D.S. (1959) *Physicochemical basis of the analysis of the paragenesis of minerals.* New York Consult. Bur. Inc., Chapman & Hall, London, 142 p.

Lasaga, A.C. (1981) The atomistic basis of kinetics: defects in minerals. In *Kinetics of Geochemical Processes* (A.C. Lasaga and R.J. Kirkpatrik, eds), *Reviews in Mineralogy*, **8**, Mineralogical Society of America, Washington D.C., pp. 261–319.

Losert, J. (1968) On the genesis of nodular sillimanite rocks. *23rd Int. Geol. Congr.*, **4**, 109–22.

Orville, P.M. (1962) Alkali metasomatism produced by alkali ion exchange within a thermal gradient. *Geol. Soc. Amer., Spec. Pap.*, **243**.

Pascal, M.L. (1984) *Nature et propriétés des espèces en solution dans le système K_2O-Na_2O-SiO_2-H_2O-HCl: contribution expérimentale.* Thèse de Doctorat d'état, Université Pierre et Marie Curie.

Poty, B. (1969) La croissance des cristaux de quartz dans les filons sur l'exemple du filon de la Gardette (Bourg d'Oisans) et des filons du massif du Mont Blanc. *Mem. 17, Sciences de la terre, Nancy.*

Poinssot, C., Goffé, B., Magonthier, M.-C. and Toulhoat, P. (1996) Hydrothermal alteration of a simulated nuclear waste glass: effects of a thermal gradient and of a chemical barrier. *Eur. J. Mineral.*, **8**, 533–48.

Robert, C. and Goffé, B. (1993) Zeolitization of basalts in subaqueous freshwater settings: Field observations and experimental study. *Geochim. Cosmochim. Acta*, **57**, 3597–612.

Rubenach, M.J. and Bell, T.H. (1988) Microstructural controls and the role of graphite in matrix/porphyroblast exchange during synkinematic andalusite growth in a granitoid aureole. *J. metam. Geol.*, **6**, 651–66.

Sauniac, S. and Touret, J. (1983) Petrology and fluid inclusions of a quartz-kyanite segregation in the main thrust zone of the Himalaya. *Lithos*, **16**, 35–45.

Schott, J. (1973) *Contribution à l'étude de la thermodiffusion dans les milieux poreux. Application aux possibilités de concentrations*

naturelles. Thèse Doctorat d'Etat (Sciences), Université P.-Sabatier, Toulouse.

Thornton, E.C. and Seyfried, W.E. (1983) Thermodiffusional transport in pelagic clay: implications for nuclear waste disposal in geological media. *Science*, **20**, 1156–8.

Tuttle, O.F. (1949) Two pressure vessels for silicate-water studies. *Bull. Geol. Soc. Amer.*, **60**, 1727–9.

Vard, E. and Williams-Jones, A.E. (1993) A fluid inclusion study of vug minerals in dawsonite-altered phonolite sills, Montreal, Quebec: implications for HFSE mobility. *Contrib. Mineral. Petrol.*, **113**, 410–23.

Vidal, O. (1997) Experimental study of the thermal stability of pyrophyllite, paragonite, and clays in a thermal gradient. *Eur. J. Mineral.*, **9**, 123–40.

Vidal, O., Magonthier, M.-C., Joanny, V. and Creach, M. (1995) Partitioning of La between solid and solution during the ageing of Si-Al-Fe-La-Ca gels under simulated near-field conditions of nuclear waste disposal. *Appl. Geochem.*, **10**, 269–84.

Vidal, O. and Murphy, W.M. (1999) Calculation of the effect of gaseous thermodiffusion and thermogravitation processes on the relative humidity surrounding a high level nuclear waste canister. *Waste Management*, **19**, 189–98.

Walther, J.V. (1986) Mineral solubilities in supercritical H_2O solutions. *Pure Appl. Chem.*, **58**, 1585–98.

Watson, E.B. and Wark, D.A. (1997) Diffusion of dissolved SiO_2 in H_2O at 1 Gpa, with implications for mass transport in the crust and upper mantle. *Contrib. Mineral. Petrol.*, **130**, 66–80.

Woodland A.B. and Walther, J.V. (1987) Experimental determination of the solubility of the assemblage paragonite, albite, and quartz in supercritical H_2O. *Geochim. Cosmochim. Acta*, **51**, 365–72.

Yardley, B.W.D. (1977) The nature and the significance of the mechanism of sillimanite growth in the Connemara schists, Ireland. *Contrib. Mineral. Petrol.*, **65**, 53–8.

[*Manuscript received 5 August 1998: revised 9 February 1999*]

Appendix

Calculation of the solution composition at 550 and 400°C

All calculations were made using ideal activity models for all aqueous species, and assuming that H_4SiO_4, $Al(OH)_3$, $KAl(OH)_4$, KOH, K^+, H^+ and OH^- were the only aqueous species present in our experiments. Kyanite was assumed to be the phase crystallizing at the HE of GRL1 and GRL14. This hypothesis may be false for GRL1, but the results of calculation are at least qualitatively the same if andalusite is used instead of kyanite. Before it was completely removed from the capsule at the HE, quartz was present at both ends of the tubes, so that (mH_4SiO_4) corresponds to the quartz solubility in pure water. The molality of uncomplexed aluminium was calculated as: $m(Al(OH)_3)_{MKQ} = m(Al(OH)_3)_{Crn} / a(^{Crn}_{Al_2O_3})_{MKQ}$, where $m(Al(OH)_3)_{Crn}$ is the solubility of corundum in pure water (Table 2) and $a(^{Crn}_{Al_2O_3})_{MKQ} = \exp(-\Delta G_{E1}/RT - \ln a\text{Ky})$ was calculated from the following equilibrium

$$\text{Ky} = \text{Crn} + \text{Qtz} \qquad \text{(E1)}$$

The $K^+/H^+ = \exp(-\Delta G_{E2}/RT - 1.5\ln a\text{Ky})$ ratio was calculated using the variation of the Gibbs free energy for the equilibrium

$$H^+ + \text{Ms} = 1.5\ \text{Ky} + 1.5\ \text{Qtz} + K^+ + 1.5\ H_2O \qquad \text{(E2)}$$

H^+ and K^+ concentrations were then calculated combining the electroneutrality condition and the dissociation constant of H_2O. The KOH concentration was calculated using the H^+ and K^+ concentrations estimated above and the dissociation constant for KOH. Finally, $KAl(OH)_4$ molality was calculated from the following expression:

$$KAl(OH)_4 = \frac{p}{p-1}\left(\frac{Al(OH)_3}{p} - KOH - K^+\right)$$

derived from the following set of equalities:

$$\text{Kt} = KAl(OH)_4 + KOH + K^+$$
$$\text{Alt/Kt} = p$$
$$\text{Alt} = Al(OH)_3 + KAl(OH)_4$$

where Alt and Kt are the total Al and K molalities, respectively.

The Gibb's free energy variation ΔG_{E1} and ΔG_{E2} (Table 2) as well as the quartz solubility were computed using the TWEEQU software (Berman, 1991) with its implemented database JAN92.RGB. Kyanite activity was unity at the HE of GRL1 and GRL14 and at the HE of GRL1. It was <1 at the CE of GRL1, where only muscovite + quartz crystallized. It was estimated for $p_{550°C} = 0.85$ and $p_{400°C} = 0.6$ (see text), in order to obtain:

$$(Alt_{550°C} - Alt_{400°C})/(Kt_{550°C} - Kt_{400°C}) = 3$$

This equality assumes that the crystallization of muscovite (Al/K = 3) is restricted to the CE and results from the variation of Al and K concentration between 550 and 400°C. This assumption is justified by the fact that except for amorphous silica, no solid was observed in the middle part of

the tubes. In doing so, we can estimate the composition of the solution equilibrated with muscovite and quartz at the CE of GRL1.

Calculation of the amount of dissolved and precipitated solids

Using the composition at 550°C, it is possible to estimate the variation in the proportion of muscovite and kyanite associated with the dissolution of quartz through the reaction:

$$\text{Starting mixture} \rightarrow a\text{Ky} + b\text{Ms} + S(\text{solution})^{550^\circ\text{C}}_{\text{MKQ}} \quad \text{(R1)}$$

Since no solid (except amorphous silica precipitated during quenching) formed in the middle part of the tube, crystallization of muscovite and quartz at the CE of GRL1 was assumed to result from the reaction

$$S(\text{solution})^{550^\circ\text{C}}_{\text{MKQ}} \rightarrow c\text{Ms} + d\text{Qtz} + S(\text{solution})^{400^\circ\text{C}}_{\text{MQ}} \quad \text{(R2)}$$

whereas for GRL14, it was assumed to result from the reaction:

$$S(\text{solution})^{550^\circ\text{C}}_{\text{MKQ}} + e\text{Ky} \rightarrow c\text{Ms} + d\text{Qtz} + S(\text{solution})^{400^\circ\text{C}}_{\text{MKQ}} \quad \text{(R3)}$$